

Port hamiltonian modeling of MSMA based actuator: toward a thermodynamically consistent formulation [★]

N. Calchand,^{*} A. Hubert,^{*} Y. Le Gorrec^{*}

^{*} *FEMTO-ST / AS2M 24, rue Alain Savary, 25000 Besançon, France
(e-mail: Yann.Le.Gorrec@ens2m.fr).*

Abstract: This paper presents a thermodynamically consistent model of MSMA (Magnetic Shape Memory Alloys) under port Hamiltonian framework. It is based on previous works on MSMA proposed in (Gauthier et al., 2008; Calchand et al., 2011). The main difference lies in the choice of the state variables and manipulated thermodynamic forces. Furthermore in (Gauthier et al., 2008), subsequent experiments revealed a highly hysteretic behavior of these materials. Here, the simplified hysteretic behavior is incorporated into the port-hamiltonian model to obtain a finer and more precise model. Such modeling will allow the use of a wide range of energy based methods to design the associated control system. The paper ends with some extensions to more complex hysteretic phenomena by using Preisach like model. First ideas are proposed to extend the previous physical model to systems with internal hysteretic loops.

Keywords: Irreversible thermodynamics, hysteresis, dissipative port Hamiltonian systems

1. INTRODUCTION

Actuators miniaturization is fast becoming essential in today's world due to their low cost, high integration capabilities and their high precision. Active materials such as piezoelectric materials or magnetostrictive materials play a major role in reducing component size. But more recently, another material called Magnetic Shape Memory Alloys (MSMA) has emerged. It offers more displacement than piezoelectric material and operate at higher speed than classical Shape Memory Alloys. MSMA, as its name suggests, uses a magnetic field to deform its shape and hence achieve displacement. Even if MSMA presents some very interesting characteristics from an application point of view, it also has complex behavior as its dynamics are driven by the irreversible thermodynamics laws. Indeed the crystal magnetization and orientation with respect to the applied magnetic field, temperature and external stress are non linear and hysteretic. Such materials are now well studied regarding their static behavior but the modeling of their dynamic behavior remains an open problem, especially from the control point of view.

A first modeling within the port-hamiltonian (Van der Schaft, 2006) framework had been done in (Calchand et al., 2011) by using analogies with mechanical systems. In this paper we propose a thermodynamically consistent model of MSMA in the port Hamiltonian formalism. For that purpose we use an internal "thermodynamic" variable associated with the crystal composition and derive the geometric structure such that the Clausius Duhem inequality

is satisfied i.e. the natural dissipation due to crystal re-orientation appears explicitly in the geometric structure. The hysteretic behavior of the material appears through the link between the thermodynamic force associated with this internal state variable and its dynamics.

The paper is organized as follows. We start by describing the MSMA based actuator we are interested in. We then focus on the MSMA, by first providing some general properties and some explanation on how a thermodynamic model can be derived. We then explain how to chose the appropriate state variables and thermodynamic forces such that the system can be derived under dissipative port Hamiltonian format. We end the paper by considering some extensions with respect to the hysteretic behavior of the system.

2. DESCRIPTION OF MSMA AS ACTUATOR

The MSMA based actuator considered in this paper is a simple device described in (Gauthier et al., 2008). As depicted in Fig. 1, it is constituted by four components: (i) a control/supply electronic device (control board + PWM power supply, not depicted on the Fig. 1), (ii) a magnetic field generation device (coil + core), (iii) a MSMA sample and (iv) a mechanical load.

For the purposes of this paper, the *magnetic field generation* part will not be considered. It will be assumed that the MSMA can be directly controlled through the resulting applied voltage u_m inducing the magnetic field (cf. Calchand et al. (2011)). Later using interconnections, the different parts will be connected together. Furthermore in a first instance we consider the isothermal case meaning that MSMA is only subject to magnetic field and external stress.

[★] The contribution of authors has been done within the context of the French National Research Agency sponsored project HAMEC-MOPSYS number ANR-11-BS03-0002. Further information is available at <http://www.hamecmopsys.ens2m.fr/>.



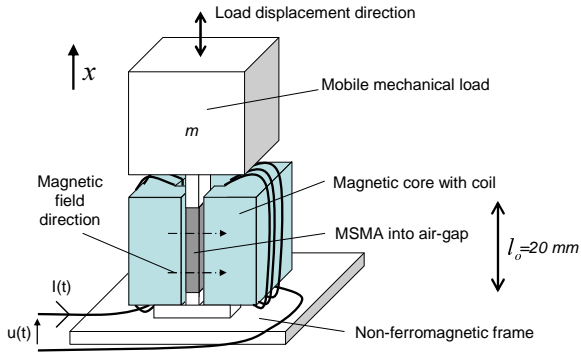


Fig. 1. Simple MSMA Actuator.

3. MSMA PROPERTIES AND CHARACTERISTICS

MSMA is an alloy of Ni_2MnGa and can be seen as a mixture of classic Shape Memory Alloy (SMA) and magnetostrictive material. In short, the microscopic behavior of MSMA is similar to the one of SMA (Bhattacharya, 2003; Lagoudas, 2008) but strain can not only be due to a martensite/austenite phase transformation but also due to a martensite reorientation under magnetic fields. In this second mode of working – martensite rearrangement –, MSMA can be assimilated to magnetostrictive materials (Terfenol-D) (du Tremolet de Lacheisserie, 1993) except that it presents a much larger magneto-mechanical coupling (6 % of maximal strain for Ni_2MnGa instead of 0.16 % for Terfenol-D). The magnetic actuation significantly increases the dynamical bandwidth of the crystallographic changes because it uses a magneto-mechanical energy conversion process instead of a thermo-mechanical process for *classical* SMA actuation. Since the first results fifteen years ago, MSMA materials have known some important improvements, namely the working temperature range and the maximum available strain. When actuated by magnetic fields, these materials now allow a large strain (up to 6 %) with a response-time in the range of milliseconds as compared to tenth of seconds or even seconds for SMA (see (Söderberg et al., 2005; Pons et al., 2008) for reviews). Currently, the most used MSMA are non-stoichiometric Ni_2MnGa monocrystals but a lot of studies are also being conducted on thin films deposition and polycrystal samples (Kohl et al., 2006, 2007). Nevertheless, these latter types are less adequate for actuation applications because of a lower magneto-mechanical coupling. In this paper, only Ni_2MnGa monocrystal is considered.

In this alloy, the martensite phase can appear in three different martensitic *variants* corresponding to the three possible crystallographic directions in the sample (see Fig. 2 (a)). At high temperature, the MSMA sample is in austenitic phase (A) but after a cooling process, the austenite phase is transformed into a martensite phase without any favoured variants (M1, M2 and M3). If a mechanical stress is applied in a specific direction, then the fraction of variant with its short axis in this direction grows. If this stress is high enough then the sample will only contain this variant (for example M2 in Fig. 2 (b)). If the stress decreases, the volume fraction of the M2 variant will also decrease but with a large thermo-magneto-mechanical hysteresis. In a similar way,

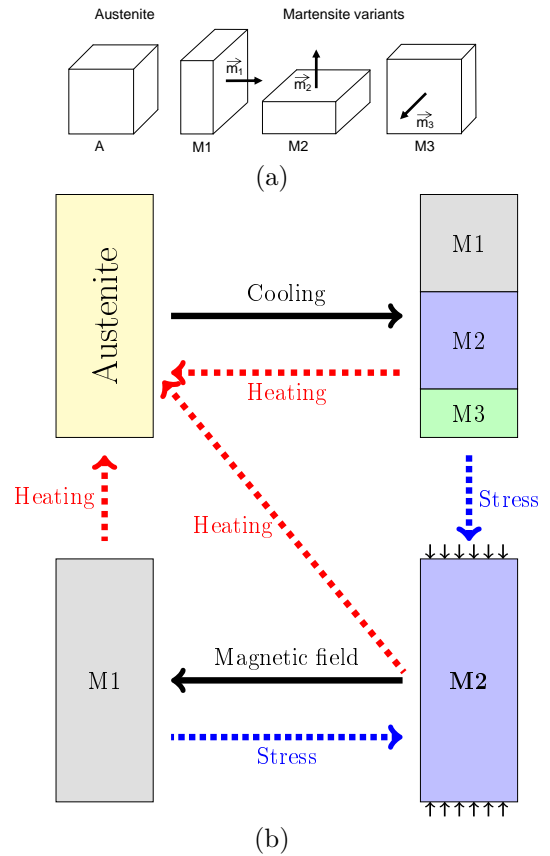


Fig. 2. MSMA Behaviour: (a) Austenite phase and the 3 martensite variants, (b) Martensitic reorientations: Effects of mechanical stress, magnetic field and temperature.

if a magnetic field is applied, the variant with its easy magnetization direction in the field direction, is favoured. For Ni_2MnGa MSMA, the easy magnetization direction is the same as the short axis of the martensite variant. In Fig. 2 (b), if magnetic and stress fields are orthogonal, they both favour a different variant of martensite (M1 or M2). The distribution between the magnetic field and the mechanical stress allows then to control the macroscopic strain. With a mechanical pre-stress, it is also possible to design an actuator driven by the magnetic field only. It should be stressed that by heating, austenite phase is recovered. More details about the structural properties of MSMA can be found in (Söderberg et al., 2005).

4. THERMODYNAMICS MODEL

Thermodynamics of irreversible processes has been used to model the MSMA in (Gauthier et al., 2007) and an overview with some extensions are proposed here. The MSMA is submitted to an external voltage inducing a magnetic field B . As only isothermal and isobaric MSMA are considered in this work, we use the free Gibbs energy for the modeling. As state variables we chose the extensive variables associated with the magnetic field *i.e.* the magnetic flux ϕ , the crystallographic composition *i.e.* the martensite variant volume fraction and two geometrical variables associated with crystallographic orientation z, θ, α , and the mechanical properties *i.e.* the strain. The free Gibbs energy density function can be then written:

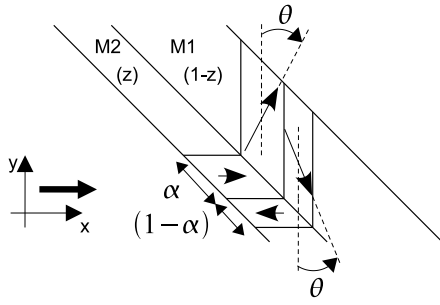


Fig. 3. Elementary volume of MSMA.

$$\check{\mathcal{G}} = \check{\mathcal{G}}(\phi, z, \theta, \alpha, \varepsilon) \quad (1)$$

As shown in Fig 3, internal variables α , θ and z have been used to model the behavior of the material. z corresponds to the martensite variant volume fraction and inside each elementary volume there are two Weiss domains. α corresponds to width of one domain with respect to the other whereas θ corresponds to the angle between the natural magnetic direction and the real direction of magnetization inside the M2 variant. On increasing the magnetic field to which the MSMA is subjected, α increases linearly until the other domain disappears and θ rotates in such a way so as to align itself with the direction of the magnetic field. It allows to take into consideration the saturation of the material. α and θ being function only of the applied magnetic field and being assumed to be reversible they are such that

$$\frac{\partial \check{\mathcal{G}}}{\partial \theta} = \frac{\partial \check{\mathcal{G}}}{\partial \alpha} = 0 \quad (2)$$

θ, α can be then derived from the other considered variables from:

$$\alpha = \frac{\chi_a H_0}{2M_s} + \frac{1}{2}, \quad \alpha \in [0, 1]$$

and

$$\sin \theta = \frac{\chi_t H_0}{M_s}, \quad \theta \in \left[-\frac{\pi}{2}, \frac{\pi}{2}\right]$$

in order to take into consideration the saturation of the material. The considered MSMA sample is a parallelepiped of length l_0 , cross section A . S is the surface perpendicular to the magnetic field and parallel to the stress and V the total volume $V = l_0 A$. Then the flux is $\phi = SB$, with B being the magnetic field. The Gibbs free energy density can be written $\check{\mathcal{G}} = \check{\mathcal{G}}(\phi, z, \varepsilon)$ and from the Gibbs equation:

$$d\check{\mathcal{G}} = \frac{H}{S} d\phi + \sigma d\varepsilon - \pi^z dz \quad (3)$$

where H is the

It has been shown in (Gauthier et al., 2008) that the total free Gibbs energy density can be written as:

$$\begin{aligned} \check{\mathcal{G}}(\varepsilon, \phi, z) = & -\frac{E}{2}(\varepsilon - \gamma z)^2 + K_{12}z(1-z) \\ & - \mu_0 M_s \left[z(2\alpha - 1)H_0 - \frac{M_s}{2\chi_a}(2\alpha - 1)^2 \right. \\ & \left. + (1-z)\left(\sin\theta H_0 - \frac{M_s}{2\chi_t}\sin^2(\theta)\right) \right] \quad (4) \end{aligned}$$

where z is the internal variable which defines the proportion of M1 in the MSMA sample and $(1-z)$ is the proportion of M2.

The conjugate variable associated with the strain (*i.e.* the stress) is given by:

$$\sigma = \frac{\partial \rho \check{\mathcal{G}}}{\partial \varepsilon} = \gamma E(\varepsilon - \gamma z) \quad (5)$$

and the thermodynamic force associated with z is then given by:

$$\begin{aligned} \pi^z = & -\frac{\partial \rho \check{\mathcal{G}}}{\partial z} = -\gamma E(\varepsilon - \gamma z) - K_{12}(1-2z) \\ & + \mu_0 M_s \left(\frac{(1-2\alpha)\sin\theta}{\chi_t} + \frac{(1-2\alpha)^2}{2\chi_a} + \frac{\sin^2\theta}{2\chi_t} \right) \quad (6) \end{aligned}$$

From a dynamical point of view, dynamics on variables ϕ and ε can be derived from conservation laws. The dynamic law associated with z is derived from experiments (Gauthier et al., 2008) and thermodynamic considerations. First the law is fitted to satisfy the hysteretic behavior of the material and such that it satisfies the Clausius-Duhem dissipation inequality. A first interpolation law has been chosen to fit with the external loop hysteretic behavior (cf Figure 4).

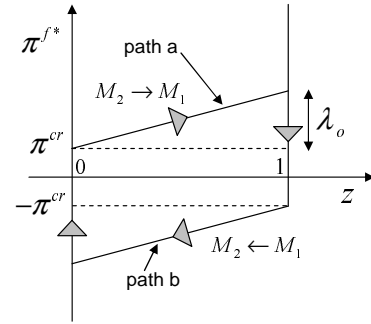


Fig. 4. External hysteresis Loop

From the figure, it is seen that the rearrangement begins only after the thermodynamic force (π^z) reaches a critical point called π_{cr}^z . Afterward z follows linearly π^z . If the thermodynamic force is reversed, the state variable move only after that π^z has reached a new critical value with then a negative dynamics. In both case one can check that the Clausius-Duhem inequality is satisfied, that is to say:

$$\pi^z \dot{z} \geq 0 \quad (7)$$

that means that the second law of thermodynamics is satisfied. A more complex dynamics on z can be chosen as it is done for example in Figure 5.

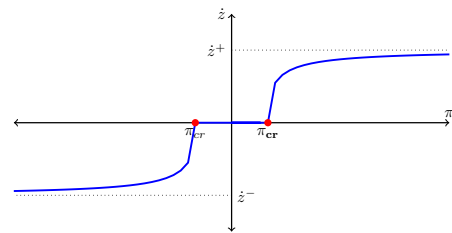


Fig. 5. Dynamics on \dot{z}

Again this hysteretic behavior obeys the Clausius-Duhem law. The system being dissipative, it has the required

properties to apply energy methods like passivity and port-hamiltonian control (Van der Schaft, 2006).

5. INTERCONNECTION WITH LOAD

As stated above, on application of a magnetic field, an elongation of the MSMA occurs. As the magnetic field is homogeneous along the MSMA sample we consider the stress is homogeneous. The load attached to it serves to apply a pre-stress on the material and returns it to its original position on removal of the magnetic field. Considering that there is always contact between the load and the MSMA, the interconnexion occurs through continuity of flux variables and equality of effort variables. If F is the force acting on the area A of the load, l_0 is the length of the MSMA and \dot{x} the velocity of the load then:

$$\begin{aligned} F &= - \int_A \sigma ds = -\sigma A \\ \dot{x} &= \int_l \dot{\epsilon} dl = l_0 \dot{\epsilon} \end{aligned} \quad (8)$$

By Newton second law, we then have the following equations:

$$m\ddot{x} = -mg - f\dot{x} + F \quad (9)$$

Defining $p_\epsilon = \frac{ml_0}{A}\dot{\epsilon}$ we can write:

$$\dot{p}_\epsilon = -\frac{mg}{A} - \frac{fl_0}{A}\dot{\epsilon} + \frac{F}{A} \quad (10)$$

where m is the mass of the load and f is the viscous friction.

6. PORT-HAMILTONIAN MODEL

The aim of this section is to recast the "MSMA+Load" system into a *pseudo* port Hamiltonian format *i.e.* system of the form:

$$\begin{aligned} \dot{x} &= (\mathcal{J} - \mathcal{R}) \delta_x \mathcal{H} + \mathcal{B}u \\ y &= \mathcal{B}^T \delta_x \mathcal{H} \end{aligned}$$

with $\delta_x \mathcal{H}$ the variational derivative of \mathcal{H} , \mathcal{J} skewsymmetric and \mathcal{R} symmetric non negative. The choices of state, flow and effort variables are summarized in Table 1.

	state	flux	effort
Mechanical load	ϵ, p_ϵ	$\dot{\epsilon}, \dot{p}_\epsilon$	$\frac{mg}{A} + \sigma, \dot{\epsilon}$
MSMA(thermodynamic)	z	\dot{z}	$-\pi^z$
MSMA(Magnetic)	ϕ	$\dot{\phi}$	i_m

Table 1. State, flow and effort variables.

The deformation of the MSMA sample causes the load applied to the msma to move. Taking m to be the mass of the load, the total energy for the system, consisting of the MSMA sample and the load can be written as:

$$\begin{aligned} \mathcal{H}(\epsilon, \phi, z) &= \int_v \left(\frac{E}{2} (\epsilon - \gamma z)^2 + K_{12} z (1 - z) \right. \\ &\quad \left. - \mu_0 M_s \left[z (2\alpha - 1) H_0 - \frac{M_s}{2\chi_a} (2\alpha - 1)^2 \right. \right. \\ &\quad \left. \left. + (1 - z) \left(\sin\theta H_0 - \frac{M_s}{2\chi_t} \sin^2(\theta) \right) \right] + \frac{1}{2} \frac{A}{l_0} \frac{p_\epsilon^2}{m} + mg \frac{\epsilon}{A} \right) dv \end{aligned} \quad (11)$$

where the input is ϕ and p_ϵ is the momentum of the load. From the state, intensive and extensive variables, the port-hamiltonian model can then be written as in equation (16).

$$\begin{bmatrix} \dot{\phi} \\ \dot{z} \\ \dot{\epsilon} \\ \dot{p}_\epsilon \end{bmatrix} = \begin{bmatrix} 0 & 0 & 0 & 0 \\ 0 & R(\pi^z) & 0 & 0 \\ 0 & 0 & 0 & 1 \\ 0 & 0 & -1 & -\frac{fl_0}{A} \end{bmatrix} \begin{bmatrix} i_m \\ -\pi^z \\ \frac{mg}{A} + \sigma \\ \dot{\epsilon} \end{bmatrix} + \begin{bmatrix} 1 \\ 0 \\ 0 \\ 0 \end{bmatrix} u_m \quad (12)$$

With output defined as:

$$i_m = [1 \ 0 \ 0 \ 0] \begin{bmatrix} i_m \\ -\pi^z \\ \frac{mg}{A} + \sigma \\ \dot{\epsilon} \end{bmatrix} \quad (13)$$

The function $R(\pi^z)$ expresses the hysteretic behavior of the material and provides the dynamic on z . In the simplest case with external loop of Figure 4 $R(\pi^z)$ is obtained by deriving with respect to time:

$$z = \begin{cases} \lambda_0 \pi^z & \text{for } \pi^z > \pi_{cr} \\ \lambda_0 \pi^z & \text{for } \pi^z < -\pi_{cr} \\ 0 & \text{elsewhere} \end{cases}$$

where π^z is given by 6 giving rise to implicit relation on z . In the case of Figure 5 the formulation is explicit:

$$R(\pi^z) = \begin{cases} \frac{\dot{z}^+}{\pi^z} \left(1 + \left(\frac{1}{(\pi^z - \pi_{cr}^+)} \right)^{\frac{-1}{p}} \right) & \text{for } \pi^z > \pi_{cr}^+ \\ \frac{\dot{z}^-}{\pi^z} \left(1 + \left(\frac{1}{(\pi_{cr}^- - \pi^z)} \right)^{\frac{-1}{p}} \right) & \text{for } \pi^z < \pi_{cr}^- \\ 0 & \text{elsewhere} \end{cases} \quad (14)$$

In both cases $\pi^z \dot{z} > 0$ is satisfied and the power balance equation can be written:

$$\frac{d\mathcal{H}}{dt} = \frac{\partial \mathcal{H}^T}{\partial x} \frac{\partial x}{\partial t} = i_m u_m - R(\pi^z) \dot{z} - \frac{fl_0}{A} \dot{\epsilon}^2 \leq i_m u_m \quad (15)$$

leading to passivity properties.

7. TOWARD MORE COMPLEX HYSTERESIS

When hysteretic behavior with internal loops is considered, the models proposed through the functions of Figure 4 or 5 are not sufficient. In this case it is possible to use more sophisticated models such as Preisach model for example. It is based on the weighed sum of canonical relays as shown in Figure 6.

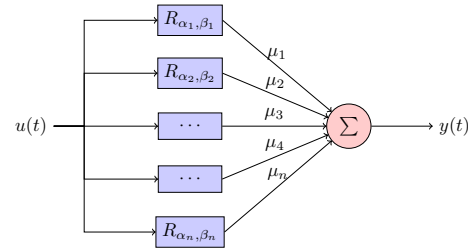


Fig. 6. Paralell connection of relays give rise to the Preisach Model. Each relay has different thresholds α_i, β_i and weightings μ but they have the same input, $u(t)$ and function independently of each other (different α and β). The output of the model $y(t)$ is given by the weighted sum of the outputs of the relays.

Each relay, named *hysteron*, is characterized by two variables α, β as shown in Figure 7.

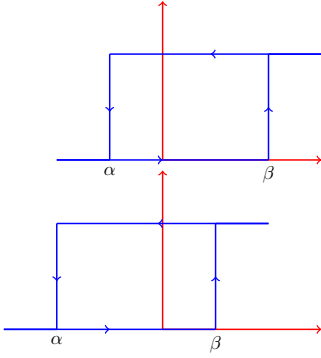


Fig. 7. Hysteron. This is the simplest hysteretic unit characterized by threshold values $\alpha < \beta$. The output takes one of the two values 0 and 1. Either it is swichted on or off.

Then it is possible to identify each threshold and weighting function through experiments. The main drawback of such approach is the loss of physical interpretation of the manipulated variables. A possible thermodynamic consistent approach of our model is to consider as many internal state variables z_i that are necessary to cope with the internal hysteretic behavior. Let us illustrate such extension with two internal variables z_1 and z_2 . The port Hamiltonian model would become:

$$\begin{bmatrix} \dot{\phi} \\ \dot{z}_1 \\ \dot{z}_2 \\ \dot{\varepsilon} \\ \dot{p}_\varepsilon \end{bmatrix} = \begin{bmatrix} 0 & 0 & 0 & 0 & 0 \\ 0 & R_1(\pi_1^z) & 0 & 0 & 0 \\ 0 & 0 & R_2(\pi_2^z) & 0 & 0 \\ 0 & 0 & 0 & 0 & 1 \\ 0 & 0 & 0 & -1 & -\frac{fl_0}{A} \end{bmatrix} \begin{bmatrix} i_m \\ -\pi_1^z \\ -\pi_2^z \\ \frac{mg}{A} + \sigma_{12} \\ \dot{\varepsilon} \end{bmatrix} + \begin{bmatrix} 1 \\ 0 \\ 0 \\ 0 \\ 0 \end{bmatrix} u_m \quad (16)$$

with efforts variables $\pi_1^z, \pi_2^z, \sigma_{12}$ derived from the total energy:

$$\begin{aligned} \mathcal{H}(\varepsilon, \phi, z_1, z_2) = & \int_v \left(\frac{E}{2} (\varepsilon - \gamma(z_1 + z_2))^2 + K_{12}^1 z_1 (1 - z_1) \right. \\ & + K_{12}^2 z_2 (1 - z_2) + \mu_0 M_s \left[z_1 (2\alpha_1 - 1) H_0 - \frac{M_s}{2\chi_a} (2\alpha_1 - 1)^2 \right. \\ & \left. \left. + (1 - z_1) \left(\sin\theta_1 H_0 - \frac{M_s}{2\chi_t} \sin^2(\theta_1) \right) \right] \right. \\ & \left. + \mu_0 M_s \left[z_2 (2\alpha_2 - 1) H_0 - \frac{M_s}{2\chi_a} (2\alpha_2 - 1)^2 \right. \right. \\ & \left. \left. + (1 - z_2) \left(\sin\theta_2 H_0 - \frac{M_s}{2\chi_t} \sin^2(\theta_2) \right) \right] \right) + \frac{1}{2} \frac{A}{l_0} \frac{p_\varepsilon^2}{m} + mg \frac{\varepsilon}{A} dv \quad (17) \end{aligned}$$

It would remains to identify the hysteretic functions $R_1(\pi_1^z)$ and $R_1(\pi_1^z)$ in accordance with the Clausius Duhem inequality to entirely characterize the behavior of the system.

8. CONCLUSION AND FURTHER WORKS

In this paper we proposed the port Hamiltonian formulation of MSMA material acting on a load. We shown that the use of an internal variable z related to the crystallographic composition allows to derive a thermodynamically consistent model with a dissipation term compatible with

the Clausius-Duhem inequality and then with the second principle of thermodynamics. The dynamic behavior of z is derived to cope with the overall system dynamics and with hysteretic behavior. In a first instance hysteresis with only external loop is considered. In this case it is shown that passivity properties are satisfied. Some extensions are proposed to extend the approach to more complex hysteretic behaviors with internal loops. It remains to validate the proposed modeling against experiments and to propose some identification procedure to derive the key functions $R(z_i)$ in a systematic way.

REFERENCES

- Bhattacharya, K. (2003). *Microstructure of Martensite: Why It Forms and How It Gives Rise to the Shape-Memory Effect*. Oxford University Press.
- Calchand, N., Hubert, A., and Le Gorrec, Y. (2011). From canonical hamiltonian to port-hamiltonian modeling: Application to magnetic shape memory alloys actuators. *DSCC Conference*.
- du Tremolet de Lacheisserie, E. (1993). *Magnetostriction: Theory and Applications of Magnetoelasticity*. CRC Press.
- Gauthier, J., Hubert, A., Abadie, J., Chaillet, N., and Lexcelent, C. (2008). Nonlinear hamiltonian modelling of magnetic shape memory alloy based actuators. *Sensors and Actuators A: Physical*, 141(2), 536–547.
- Gauthier, J., Lexcelent, C., Hubert, A., Abadie, J., and Chaillet, N. (2007). Modeling rearrangement process of martensite platelets in a magnetic shape memory alloy ni2mnga single crystal under magnetic field and (or) stress action. *Journal of intelligent material systems and structures*, 18(3), 289–299.
- Kohl, M., Brugger, D., and Krevet, B. (2006). *Ferromagnetic shape memory actuator for large 2D optical scanning*.
- Kohl, M., Brugger, D., Ohtsuka, M., and Krevet, B. (2007). A ferromagnetic shape memory actuator designed for large 2d optical scanning. *Sensors and Actuators A*, 135, 92–98.
- Lagoudas, D.C. (ed.) (2008). *Shape Memory Alloys: Modeling and Engineering Applications*. Springer-Verlag.
- Pons, J., Cesari, E., Seguí, C., Masdeu, F., and Santamarta, R. (2008). Ferromagnetic shape memory alloys: Alternatives to ni-mn-ga. *Materials Science and Engineering A*, 481-482, 57–65.
- Söderberg, O., Ge, Y., Sozinov, A., Hannula, S.P., and Lindroos, V.K. (2005). Recent breakthrough development of the magnetic shape memory effect in Ni-Mn-Ga alloys. *IOP Smart Materials and Structures*, 14, 223–335.
- Van der Schaft, A. (2006). Port-hamiltonian systems: an introductory survey. 1339–1365. URL <http://doc.utwente.nl/66742/>.